Electric and magnetic phenomena observed before the volcano-seismic activity in 2000 in the Izu Island Region, Japan

S. Uyeda*†, M. Hayakawa‡, T. Nagao*, O. Molchanov‡, K. Hattori*, Y. Orihara*, K. Gotoh‡, Y. Akinaga‡, and H. Tanaka*

*Riken International Frontier Research Group on Earthquakes, Earthquake Prediction Research Center, Tokai University, 3-20-1, Orido, Shimizu 424-8610, Japan; and ‡National Space Development Agency of Japan Remote Sensing Frontier Research Group, Department of Electronic Engineering, The University of Electro-Communications, 1-5-1 Chofugaoka, Chofu 182-8585, Japan

Contributed by S. Uyeda, April 6, 2002

Significant anomalous changes in the ultra low frequency range (≈0.01 Hz) were observed in both geoelectric and geomagnetic fields before the major volcano-seismic activity in the Izu Island region, Japan. The spectral intensity of the geoelectric potential difference between some electrodes on Niijima Island and the third principal component of geomagnetic field variations at an array network in Izu Peninsula started to increase from a few months before the onset of the volcano-seismic activity, culminating immediately before nearby magnitude 6 class earthquakes. Appearance of similar changes in two different measurements conducted at two far apart sites seems to provide information supporting the reality of preseismic electromagnetic signals.

A two-month-long volcano-seismic activity started on June 26, 2000 in the Izu island region, Japan (Fig. 1). On June 26, 2000, an official alarm was issued by the Japan Meteorological Agency for imminent volcanic activity of the Miyakejima Island (Fig. 1) based on suddenly increased occurrences of small earthquakes under the island. In the next morning, at several kilometers west of the island, an undersea eruption occurred. A large seismic swarm started almost simultaneously (1). A large-scale depression at the summit of the Miyakejima volcano occurred on July 8. The depression grew, with frequent phreatic eruptions to a 550-m-deep caldera with a diameter of about 1,600 m.

The population of about 3,000 was totally evacuated, from September 4 up to the time of writing of this paper (April 4, 2002), because of the continued massive emission of toxic gases. This volcanic activity was unusual because the amount of ejecta was less than 5% of the volume of the newly formed caldera.[¶] The swarm earthquake activity rapidly migrated northwestward from Miyakejima, reaching near Kozu-shima about 30 km away in about 1 week (1). This swarm activity generated several magnitude (M hereafter) 6 class events (Fig. 1). The Global Positioning System data indicated that the distance between Kozu-shima and Niijima Island increased about 90 cm in about 2 months, and the whole swarm activity was explained in terms of northwestward migration of underground magma from beneath Miyakejima (2). Here we report the electric and magnetic phenomena that preceded this volcano-seismic activity. These phenomena were different from most of the preseismic electromagnetic signals reported so far for single events (3–5) because they lasted much longer before the onset of the volcano-seismic activity.

Geoelectric Potential Changes. A geoelectric potential-monitoring station with six long (1–6 km) and six short (about 30 m) dipoles using telephone cables was on Niijima Island (Fig. 1). The sampling rate was 10 s. Fig. 2 shows typical records of the long dipole connecting Air (Niijima Airport) and Wak (Wakago Village; Fig. 1) for a few time windows. Niijima Island usually is electrically almost noise-free, as in Fig. 2 *A* and *D*. From about 2 months before the onset of the activity on June 26, the Air–Wak long dipole and the short dipole at Wak started to show innumerable visually clear, unusual changes, consisting of semibox shape changes and oscillations of one to a few minutes (Fig. 2*B*).

The changes became more pronounced after June 26, culminating before the first nearby large earthquake (July 1, M6.4; as seen in Fig. 2*C*). The monitoring system was kept out of service from July 13 to August 16 for the power failure caused by earthquake shaking and typhoons. After the whole activity was ended, the records went back to noise-free as in Fig. 2*D*. It is strange that these anomalous changes were not observed on other dipoles in the region.

The observation above may be better represented by the following analysis. Fig. 3 shows the 3-year records of daily spectral intensity at 0.01 ± 0.0003 Hz band of the geoelectric potential difference of Wak–Air and Boe–Air long dipoles. Some rise in the spectral intensity from the late April may be noticed in Wak–Air dipole data. Changes common to Wak–Air and Boe–Air dipoles are mainly caused by geomagnetic field variations originating in the upper atmosphere. To eliminate these noises, the ratio of these two time series data were taken as shown in the upper profiles of Fig. 5 *a* and *b*. The rise before the volcano-seismic activity, the more pronounced enhancement after June 26 with a peak before the M6.4 July 1 earthquake, and the return to the noise-free situation simultaneously with the decline of the swarm activity can now be seen more clearly. The same tendency was verified for the frequency range of 0.0001–0.03 Hz, but the enhancement was strongest in the 0.006–0.03 Hz range.

Because two independent Wak dipoles (long and short), without a common electrode, showed simultaneous changes, electrode instability is an unlikely cause. Although telephone cable noise and villagers' activity could have caused the changes, it seems too coincidental that the changes occurred only during this particular time in the entire 3 years of observation. As mentioned above, of six pairs of long and short dipoles, only Wak dipoles revealed the changes. One possible factor that might have relevance to this peculiar fact is that only the Wakago area is covered by basaltic rocks, whereas the rest of the whole island is composed of rhyolitic rocks (Fig. 1). Such a geologic heterogeneity amplifying the seismic electric signals by orders of magnitude was also reported in Greece (6).

Magnetic Field Changes. As shown in Fig. 1, tripartite geomagnetic differential array networks were in both Izu and Boso Peninsulas. The spacing between stations was 5–10 km. Each station was equipped with a high-sensitive, three-component Torsion-type magnetometer (7). The sampling rates were 0.02 s at SEI and MCI and 0.08 s at KAM. Extraction of possible seismo-ultra low frequency (ULF) emissions from the array data were made through the principal component analysis (8). The north-south component

Abbreviations: M, magnitude; ULF, Ultra Low Frequency (0–100 Hz).

†To whom reprint requests should be addressed. E-mail: suyeda@st.rim.or.jp.

¶Nakada, S. & Fuji, T. (2000) *EOS Trans. AGU* **81,** 48, Suppl., Abstr. V52.A-02.

www.pnas.org/cgi/doi/10.1073/pnas.072208499

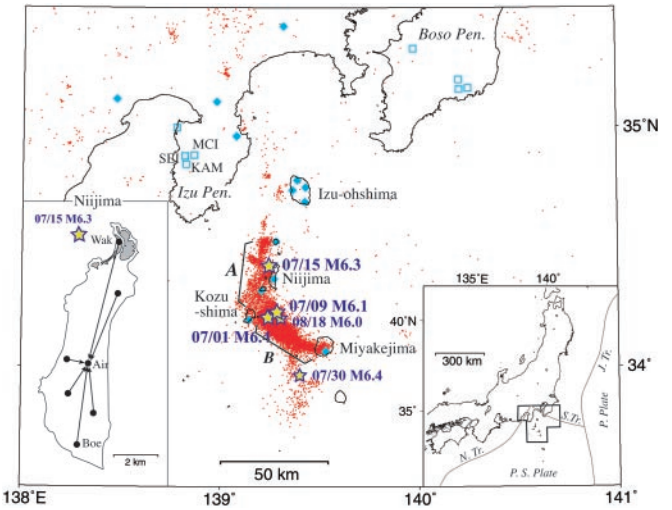

Fig. 1. Index map of the Izu island region. Red dots are M ≥ 0 earthquakes according to Japan Meteorological Agency for June 1 to September 30, 2000. Yellow stars are M ≥ 6 earthquakes. Diamonds are geoelectric stations; open squares are geomagnetic stations. Areas A and B are mentioned in the last section of the text. *Right Inset* is a map of Japan with plate boundaries. P. plate, Pacific Plate; P.S. plate, Philippine Sea Plate; N.Tr., Nankai Trough; S.Tr., Sagami Trough. *Left Inset* shows the long dipole configuration of Niijima station. A short dipole (not shown) is also installed at the far end of each long dipole centered at Air (Airport). Shaded area around Wak is covered by basalt, whereas the rest of the island consists of rhyolite.

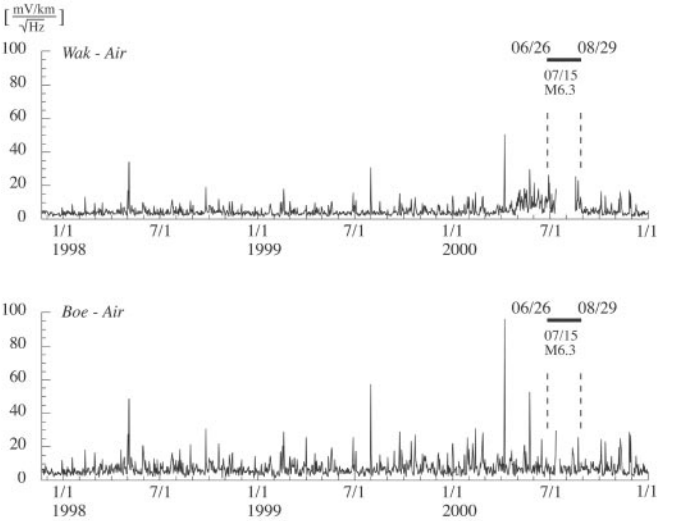

Fig. 3. Three-year record of 0.01 ± 0.0003 Hz spectral intensity of geoelectric field intensity. (*Upper*) Wak–Air dipole. (*Lower*) Boe–Air dipole. (See also Fig. 5.) The lack of data for Wak–Air dipole in the year 2000 was caused by power failure and mechanical damage caused by a typhoon and the July 15 M6.3 earthquake (star) of which epicenter was close to Wakago Village (Wak, Fig. 1). The volcano-seismic activity, starting on June 26, 2000 as shown by the vertical dotted line, lasted to August 29.

data for the whole period (1 year) of tripartite observation were used to differentiate the variations caused by different sources (geomagnetic variations, man-made noise, and other sources). The ULF waveform data sampled at 1 s were fed to into a numerical 0.01 ± 0.002 Hz bandpass filter on the basis of previous studies (9–11). By measuring the correlations between the data from the three stations, we estimated three eigen vectors and eigen values ($\lambda_1 > \lambda_2 > \lambda_3$), thereby separating three components with possibly different sources. The ith eigen value is proportional to the power of the ith principal component. Fig. 4*a* illustrates the time variation of the first principal eigen value $\sqrt{\lambda_1}$ estimated at every 30 min together with Ap index, which is commonly used to indicate the

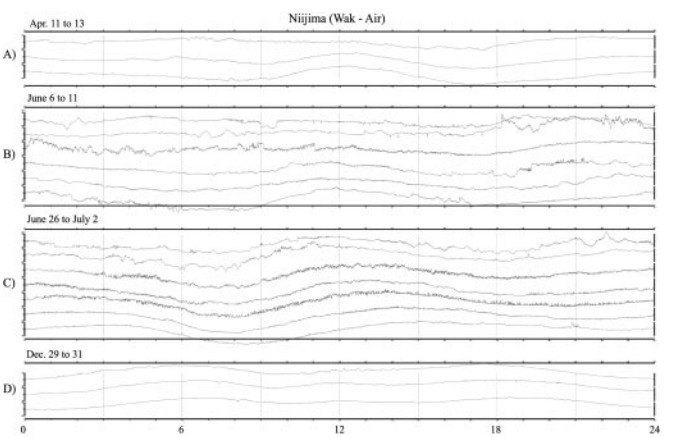

Fig. 2. Examples of typical 24-h records of Wak–Air dipole electric potential difference. (Bar on vertical axis for each day is 50 mV.) (*A*) Before April 26. Records showed mainly smooth tidal variations only. (*B*) During 2 months before the onset (June 26) of the volcano-seismic activity. Numerous anomalous changes occurred. (*C*) Just after June 26. Anomalous changes were more conspicuous. (*D*) After the cessation of the activity, records resumed usual quietness. Time windows A, B, C, and D are indicated in the upper panel of Fig. 5.

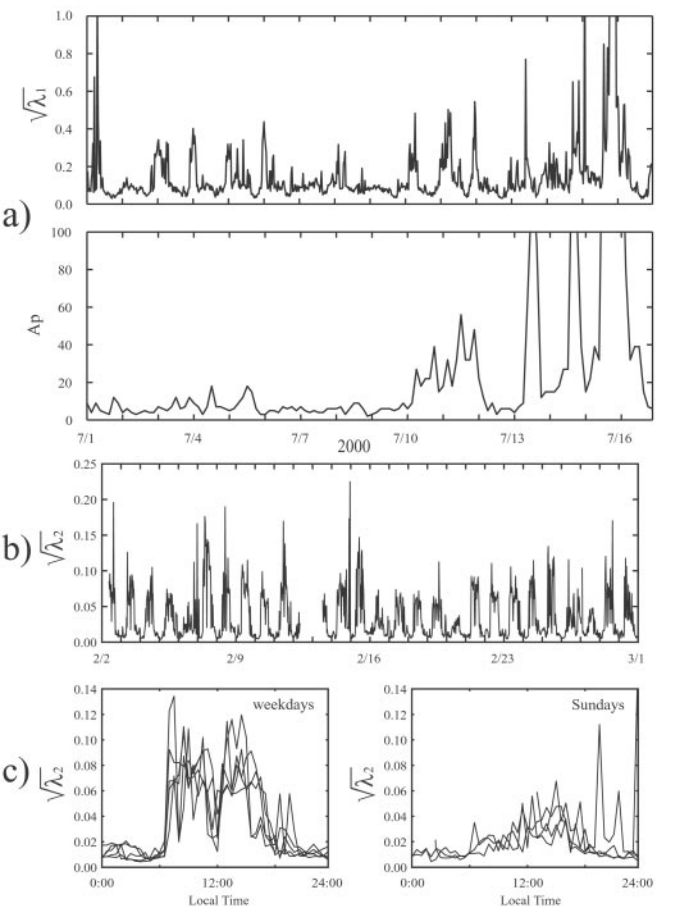

Fig. 4. (*a*) Comparison of the time change of the first principal component $\sqrt{\lambda_1}$ at 0.01 Hz with that of Ap index from July 1 to July 16, 2000. (*b*) Time change of the second principal component ($\sqrt{\lambda_2}$) during 1 month (February 2000). (*c*) The diurnal variation of $\sqrt{\lambda_2}$ on weekdays (*Left*) and Sundays (*Right*).

GEOPHYSICS

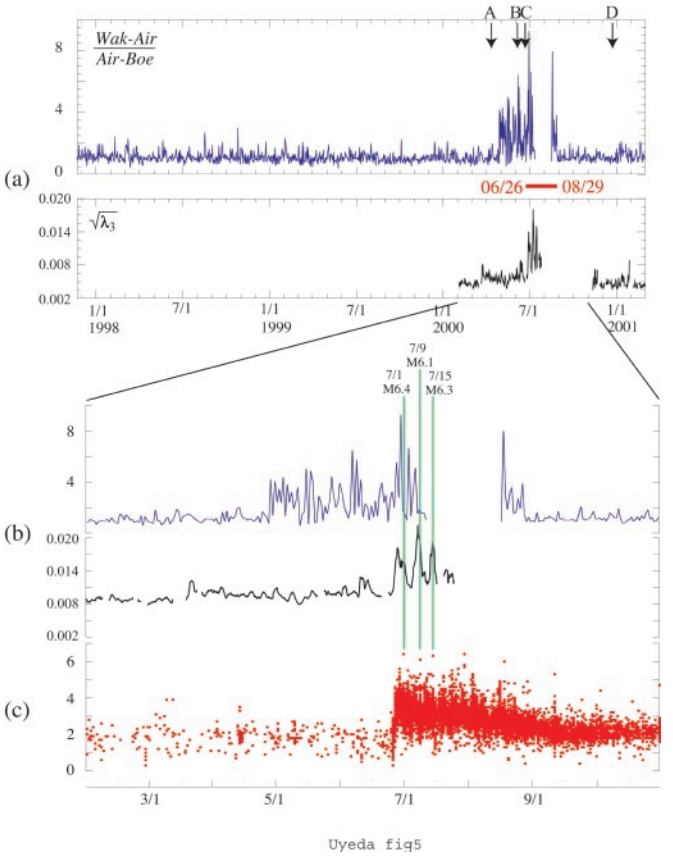

Fig. 5. Time change of the 0.01 Hz spectral intensity ratio (blue) of geoelectric potential difference at Wak–Air and Boe–Air dipoles, Niijima Island, and that of the third principal component ($\sqrt{\lambda_3}$) at 0.01 Hz of the geomagnetic field at Izu Peninsula array station (black). The gap in data was caused by system failure in July and August. (*a*) For 3-year period. (*b*) For January through October, 2000. Three M ≥ 6 earthquakes in July are indicated by vertical green lines. (*c*) Seismicity of the Izu Island region (red dots). For A, B, C, and D in *a*, see Fig. 2.

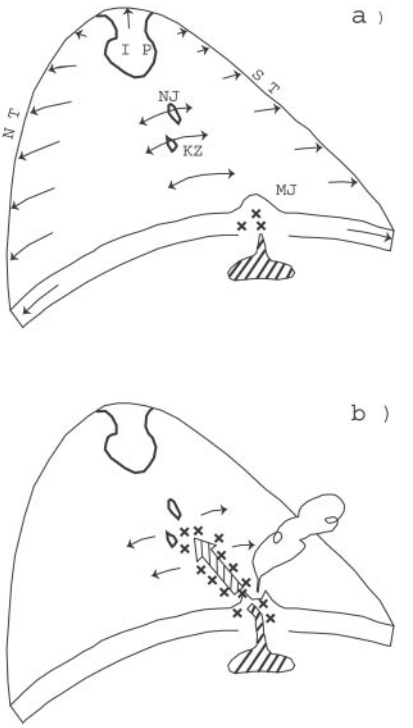

Fig. 6. Cartoon presentation of the tectonic scheme of the northeastern corner of the Philippine Sea plate. (*a*) This part of Philippine Sea plate is under northeast–southwest-oriented regional tensile stress because of subduction at Sagami Trough (ST) and eastern Nankai Trough (NT). The figure depicts that this stress regime helped magma (shaded) rise under Miyakejima (MJ) and prepared a path for the magma's subsequent passage toward Kozushima (KZ) and Niijima (NJ) area. This process was aseismic but generated electric and magnetic signatures observed at NJ and Izu Peninsula (IP). IP on Philippine Sea plate is in collision with the mainland Japan. Arrows, normal component of plate motion relative to the other side; two-sided arrows, stress; crosses, earthquakes. (*b*) After June 26, magma migrated along the prepared path causing the large-scale swarm seismicity and associated geodetic widening (arrows). Because of drainage of magma, the summit of MJ collapsed to form the caldera. Arrows common to *a* are omitted for clarity.

degree of geomagnetic disturbance caused by solar activity. This figure shows that the $\sqrt{\lambda_1}$ component is likely geomagnetic disturbance. The change of the second principal component $\sqrt{\lambda_2}$ (Fig. 4*b*) shows a regular daily variation probably related to human activity, which is better illustrated in Fig. 4*c*. During weekdays, a lunch-time effect occurs, whereas no such effect happens on Sundays. The third principal component ($\sqrt{\lambda_3}$) is the variation caused by causes other than the previous two, possibly including seismo-ULF emission if it exists. The lower profiles of Fig. 5 *a* and *b* illustrate the time change of $\sqrt{\lambda_3}$, obtained by using only the nighttime (0000–0400 local time) data. With the whole-day data, the pattern was contaminated with strong diurnal variation reminiscent of Fig. 4*b*.

The intensity of $\sqrt{\lambda_3}$ shown in Fig. 5*a* begins to increase from late March and, after a lull for about 2 weeks, the volcano-seismic activity broke out. Such a brief lull has also been noticed for ULF preseismic magnetic signals in the past (9, 10). Abrupt increase in $\sqrt{\lambda_3}$ occurred immediately before the three nearby M6 class earthquakes (lower profile, Fig. 5*b*). The level of $\sqrt{\lambda_3}$ was back to the usual background level when the volcano-seismic activity was finished. Thus, it is highly likely that the observed enhancements in $\sqrt{\lambda_3}$ were seismogenic ULF emissions. Although less pronounced, a similar tendency was obtained at the 0.1 Hz band also. The data from the Boso Peninsula array more than 100 km distant from the swarm area did not reveal similar changes.

The intensity of $\sqrt{\lambda_3}$ was about 1% and 5% of that of $\sqrt{\lambda_1}$ during the preactivity period and just before the large earthquakes, respectively. This suggests that the intensity of the possible seismogenic ULF emission was probably of the order of 10^{-1} nT or less. In the nearby M7–8 class events like the Loma Prieta earthquake (9), rather strong signals could be detected by the conventional analysis. Sometimes more detailed signal processing like polarization and fractal analysis was also used for weak signal detection (10, 12). In the present case, where the signals were expected to be weaker, the principal component analysis proved to be useful.

Concluding Remarks. In Japan, during the past several years, we have been monitoring the geoelectric potential and geomagnetic field variations and have demonstrated that apparently meaningful signals were observed depending on the magnitude and epicentral distance of earthquakes and the noise level of observing stations (e.g., refs. 4, 5, and 13); for example, both preseismic and coseismic transient geoelectric potential changes were observed for all five earthquakes with magnitudes greater than 5 that occurred within a few tens of kilometers from low-noise stations during the observation period (5, 14, 15). The lead time of the observed preseismic changes ranged from 1 to 19 days. Even in the 1995 M7.2 Kobe earthquake for which several possible electromagnetic precursors were reported (16), no simultaneous ULF electric and magnetic monitoring was

conducted. The Izu activity in 2000 provided a rare chance for this monitoring.

Izu island region of the Philippine Sea plate is under a chronic regional southwest-northeast tensile stress because of its subduction at the Nankai and Sagami Troughs (20) (Fig. 6*a* and Fig. 1 *Inset*). The historically recorded volcanic activity of the Miyakejima volcano with intervals of a few tens of years is caused by the rise of magma aided probably by this tensile tectonic stress. Our observations revealed two major electromagnetic phenomena. One was the enhanced variations during a few months before the onset (June 26) of the volcano-seismic swarm activity (stage 1), and the other was the more enhanced variations after the onset (stage 2).

The preswarm enhancement may be interpreted as a precursor to the whole swarm activity caused by the later magma migration. The amplitudes of the anomalous changes observed at this stage were of the order of 2 mV/km at Wak, Niijima Island and 10^{-1} nT or less at Izu Peninsula array. To produce the signals of these orders of magnitude, a simple uniformly conducting half-space model (17), with reasonable parameters, in which a point dipole is embedded at 10-km depth in the middle of the swarm area, indicates that the dipole intensity has to be of the order of 10^6 Am, which is expected for precursors of M5 class earthquakes (18, 19). Obviously, such a simple model cannot be applied to the present case where extreme heterogeneity of the medium is involved, as suspected from the selective appearance of signals in Niijima Island. Existence of favorable heterogeneity like conductive channels may reduce the necessary dipole intensity by a few orders of magnitude (18). However, the enhancement was not related to any observable earthquakes. M2 class background seismicity was present, as shown in Fig. 5*c*, but it is not relevant because it has been going on all of the time. Moreover, all of the epicenters were in area A in Fig. 1, and the area of the impending swarm (area B in Fig. 1) was essentially aseismic until the outbreak of the volcano-seismic activity according to Japan Meteorological Agency. Thus, the observation seems to require that, at state 1, electric currents with ULF frequency were being generated through a process without causing earthquakes observable by routine short-period seismometry. It may be speculated that this seismically silent process was generating distributed microelectric sources in the impending swarm zone by either electrokinetic or solid-state mechanisms (20–22). At stage 2, the magma, instead of erupting vertically upward, migrated horizontally northwestward along the path prepared by the tensile regional tectonic stress during stage 1. Once magma migration started, a similarly migrating strong earthquake swarm was induced, and the electric and magnetic signals became more pronounced (Fig. 6*b*).

Another important problem remains; i.e., throughout the whole process, electric signals were observed at only Wak dipoles. Here, highly conductive channels may be involved. Channels can be of various sizes. Macroscopic structures like geological heterogeneity and/or faults containing bulk water may act as conductive channels (6, 18). Even if such a favorable condition does not exist, microscopic channels may be envisaged. According to the recent studies, the stress in granular materials under load locally concentrates like roots of a plant to form the so-called "stress chains" (23). If such stress chains are formed in the crust, they may also act as conductive channels. Water molecules adsorbed to the surfaces of closely packed grains in the stress chains would form networks of clusters. Proton diffusion through such networks might dramatically enhance the electric conductivity. To verify this possibility, electrical properties of clustered water molecules must be investigated further.

Although many unexplained elements remain, as stated above, the fact that two different quantities, one geoelectric and the other geomagnetic, monitored at two far apart sites indicated similar anomalous signatures seems to provide supporting evidence for the reality of electromagnetic phenomena preceding the major regional volcano-seismic activity.

1. Japan Meteorological Agency (2000) *Earth Planets Space* **52,** i–viii.
2. Nishimura, T., Murakami, M., Ozawa, S., Sagiya, T., Yarai, H. & Imakiire, T. (2001) *Geophys. Res. Lett.* **28,** 3745–3748.
3. Varotsos, P., Lazaridou, M., Eftaxias, K., Antonopoulos, G., Makris, J. & Kopanas, J. (1996) in *A Critical Review on VAN: Earthquake Prediction from Seismic Electric Signals,* ed. Lighthill, J. (World Scientific, Singapore), pp.29–76.
4. Molchanov, O. A. & Hayakawa, M. (1998) *J. Geophys. Res.* **103,** 17489–17504.
5. Uyeda, S., Nagao, T., Orihara, Y. & Takahashi, I. (2000) *Proc. Natl. Acad. Sci. USA* **97,** 4561–4566.
6. Varotsos, P. & Lazaridou, M. (1991) *Tectonophysics* **188,** 321–347.
7. Kopytenko, Yu. A., Ismagilov, V. S., Voronov, P. M., Kopytenko, E. A. & Petlenko, A. V. (1994) in *Electromagnetic Phenomena Related to Earthquake Prediction,* eds. Hayakawa, M. & Fujinawa, Y. (Terra Scientific, Tokyo), pp. 247–252.
8. Hyvarinen, A., Karhunen, J. & Oja, E. (2001) *Independent Component Analysis* (Wiley, New York), pp. 125–144.
9. Fraser-Smith, A. C., Bernardi, A., McGill, P. R., Lad, M. E., Helliwell, R. A. & Villard, O. G., Jr., (1990) *Geophys. Res. Lett.* **17,** 1465–1468.
10. Hayakawa, M., Kawate, R., Molchanov, O. A & Yumoto, K. (1996) *Geophys. Res. Lett.* **23,** 241–244.
11. Hayakawa, M., Kopytenko, Yu. Smirnova, N., Troyan, V. & Peterson. (2000) *Phys. Chem. Earth A* **25,** 263–269.
12. Hayakawa, M., Itoh, T., Hattori, K. & Yumoto, K. (2000) *Geophys. Res. Lett.* **27,** 1531–1534.
13. Hattori, K., Akinaga, Y., Hayakawa, M., Yumoto, T., Nagao, T. & Uyeda, S. (2002) in *Seismo Electromagnetics* (*Lithosphere-Atmosphere-Ionosphere Coupling*) eds. Hayakawa, M. & Molchanov, O.A. (Terra Scientific, Tokyo), in press.
14. Orihara, Y., Noda, T., Nagao & T. Uyeda, S. (2002) *J. Geodynamics* **33,** 361–368.
15. Nagao, T., Orihara, Y., Yamaguchi, T., Takahashi, I., Hattori, K., Noda, Y., Sayanagi, K. and Uyeda, S. (2000) *Geophys. Res. Lett.* **27,** 1535–1538.
16. Nagao, T., Enomoto, Y., Fujinawa, Y., Hata, M., Hayakawa, M., Huang, Q., Izutsu, J., Kushida, Y., Maeda, K., Oike, K., Uyeda, S. & Yoshino, T. (2002) *J. Geodynamics* **33,** 349–359.
17. Banos, A. (1966) *Dipole Radiation in the Presence of a Conducting Half-Space* (Pergamon, Oxford), pp. 195–235.
18. Varotsos, P., Sarlis, N., Lazaridou, M. & Kapiris, P. (1998) *J. Appl. Phys.* **83,** 60–70.
19. Hadjikontes, V. & Mavromatou, C. (1996) in *A Critical Review on VAN: Earthquake Prediction from Seismic Electric Signals,* ed. Lighthill, J. (World Scientific, Singapore), pp. 105–117.
20. Nakamura, K., Shimazaki, K. & Yonekura, N. (1984) *Bull. Soc. Geol. France* **26,** 211–243.
21. Mizutani, H., Ishido, T., Yokokura, T. & Ohnishi, S. (1976) *Geophys. Res. Lett.* **3,** 365–368.
22. Nowick, A. S. (1996) *Annu. Rev. Mater. Sci.* **26,** 1–19.
23. Liu, C., Nagel, S. R., Schecter, D. A., Coppersmith, S. N., Majmudar, S., Naratan, O. & Witten, T. A. (1995) *Science* **269,** 513–515.